ELSEVIER

Physica A 244 (1997) 164–175

PHYSICA A

Local contacts of membranes and strings

Christin Hiergeist, Reinhard Lipowsky*

Max-Planck-Institut für Kolloid- und Grenzflächenforschung, Kantstrasse 55, D-14513 Teltow-Seehof, Germany

Abstract

Local contacts within bundles of strings and bunches of membranes are studied using transfer matrix methods, scaling theories, and Monte Carlo simulations. The contact probabilities exhibit scaling laws and decay as inverse power laws $\sim 1/\ell^{\zeta_n/\zeta}$ with increasing separation ℓ of the manifolds, where ζ denotes the corresponding roughness exponent. The contact exponents ζ_n have different values away from the boundaries of the system and close to those boundaries. These results imply that local contacts are less frequent than suggested by the widely used picture in which the fluctuation-induced interaction is interpreted in terms of collisions. In fact, deep within the bundle or bunch, one has, on average, only one pair collision per $\sim\ell$ humps.

PACS: 05.40.+j; 64.60-i; 82.70.-y

Dedicated to Ben Widom on the occasion of his 70th birthday

1. Introduction: scaling picture

Flexible membranes such as lipid bilayers in solution often form bunches or stacks in which several membranes are, on average, parallel to each other (for a recent review, see [1]). We will focus here on fluid membranes which experience an effectively repulsive interaction but cannot unbind since they are kept together by external constraints or by osmotic pressure. One experimental example is provided by charged membranes which repel each other by electrostatic forces and which exchange water with a polymer solution; see, e.g., [2]. As the osmotic pressure is decreased, the mean separation between the membranes is increased and the whole bunch is swollen.

The behaviour of the mean separation ℓ as a function of the osmotic pressure P can be obtained from scaling arguments which were originally used by Helfrich [3] for membranes between two hard walls. In order to estimate the loss of entropy which a membrane in a stack suffers from the confinement between the other membranes, this

* Corresponding author. E-mail: lipowsky@mpikg-teltow.mpg.de.

PII S0378-4371(97)00297-5

membrane is viewed as an ensemble of uncorrelated humps: each hump has a transverse extension $\xi_\perp \sim \ell$ and a lateral extension $\xi_\parallel \sim \ell$ which implies the hump volume $\mathscr{V} \sim \xi_\perp \xi_\parallel^2 \sim \ell^3$. Using the ideal gas law $P\mathscr{V} = T$ for a single degree of freedom, one then arrives at the pressure $P \sim 1/\ell^3$ (here and below, temperature is measured in energy units, i.e., the Boltzmann constant k_B has been absorbed into the symbol T). This functional dependence has been confirmed by extensive Monte Carlo simulations [4–7] and is consistent with scattering experiments on lamellar phases of oil–water–surfactant mixtures [8,9].

Let us now focus on two neighbouring membranes within such a bunch and let us ask how frequently these membranes touch each other, i.e., how often their separation lies within a fixed microscopic distance. In general, we will consider the contact probabilities $\mathscr{P}_n$ for local contacts of $n \geqslant 2$ membranes which touch each other simultaneously. As shown below, these contact probabilities $\mathscr{P}_n$ decay as $\mathscr{P}_n \sim 1/\ell^{\zeta_n}$ with characteristic contact exponents ζ_n.

It is tempting to use the aforementioned scaling picture in order to estimate the contact probability $\mathscr{P}_2$ of two adjacent membranes. Indeed, this picture seems to suggest that the entropy loss reflects the collisions or close contacts between the membranes, an interpretation which is rather widespread in the literature. This would imply that one has one collision per hump with projected area $\sim \ell^2$, and thus a contact probability which scales as $\mathscr{P}_2 \sim 1/\ell^2$. The latter relation is, however, *wrong*! As will be shown below, the correct behaviour is $\mathscr{P}_2 \sim 1/\ell^3$ which means that one has, on average, only one collision per $\mathscr{N} \sim \ell$ humps: in the limit of large ℓ, most humps do not lead to any contacts since the membranes bend back before they come close to each other.

It has been argued some time ago that the scaling behaviour of fluid membranes is quite analogous to the scaling properties of one-dimensional strings governed by a line tension (this analogy is valid as long as the interaction potentials do not exhibit a potential barrier, see [1]). Indeed, the collision picture leads to the same relation $P \sim 1/\ell^3$ between the external pressure P and the string separation ℓ which is implicitly contained in some early work on steps or ledges on crystal surfaces [10] and has been explicitly derived by Pokrovskii and Talanov for commensurate–incommensurate transitions in two dimensions [11]. Likewise, this picture leads again to the same scaling behaviour $\mathscr{P}_2 \sim 1/\ell^2$ for the contact probability of two adjacent strings. The former relation for pressure is again correct but the latter relation for the contact probability is again wrong, see below.

In the following, we will first consider a bundle of N strings between two rigid surfaces and determine the probabilities for local contacts of these strings. These probabilities exhibit scaling laws which can be obtained exactly from the well-known mapping to a system of free fermions. Using the aforementioned analogy between strings and fluid membranes, one can then make predictions for the contact probabilities of these membranes. These predictions will be confirmed below by Monte Carlo simulations for pair contacts. At the end, we give a brief outlook on related problems.

2. Bundle of N strings

Consider a bundle of N strings in two dimensions which is placed between two surfaces, i.e., two rigid boundaries as shown in Fig. 1. The Cartesian coordinates parallel and perpendicular to these surfaces are denoted by x and by z, respectively. The two surfaces are located at $z=0$ and at $z=L_\perp$. The interaction between the strings and between the strings and the surfaces is a hard-wall interaction, i.e., they are not allowed to intersect one another. The local displacement fields of the ith string from the surface at $z=0$ is denoted by l_i; these length scales satisfy $0 \leqslant l_1 \leqslant l_2 \leqslant \cdots \leqslant l_N \leqslant L_\perp$. Since there is no attractive interaction between the strings, they explore the whole space between the two surfaces, and one may define their mean separation ℓ by $L_\perp \equiv (N+1)\ell$.

2.1. Transfer matrix formalism

The partition function of such a system can be mapped, via the transfer matrix method, onto N quantum-mechanical particles. In the situation considered here in which the strings experience only hard-wall interactions, one has a system of N free fermions [12–14]. The ground state wave-function Φ_0 of such a system is obtained from the Slater determinant which is constructed from the one-particle eigenfunction $\phi_k(z)$ with $0 \leqslant z \leqslant L_\perp$. For the case considered here, these eigenfunctions must vanish at $z=0$ and $z=L_\perp$ and are thus given by $\phi_k(z)=\sqrt{2/L_\perp}\,\sin(\pi k z/L_\perp) \equiv f_k(z/L_\perp)/\sqrt{L_\perp}$, with $k=1,2,\ldots,N$. This implies the scaling form

$$\Phi_0(l_1,\ldots,l_N) = L_\perp^{-N/2} f_{N,0}(l_1/L_\perp,\ldots,l_N/L_\perp) \tag{1}$$

for the ground-state wave function. This function is taken to be normalized within the sector which corresponds to the natural ordering $0 \leqslant l_1 \leqslant l_2 \leqslant \cdots \leqslant l_N \leqslant L_\perp$.

Within the transfer matrix formalism, the probability to find the first n strings close together, i.e., the probability that these strings form a local n-contact at a certain position z is related to the quantity

$$\Phi_{0,n}(z; l_{n+1},\ldots,l_N) \equiv \Phi_0(z+a_1,\ldots,z+a_n,\ l_{n+1},\ldots,l_N)\,, \tag{2}$$

where the microscopic length scales a_k are small compared to $L_\perp$.

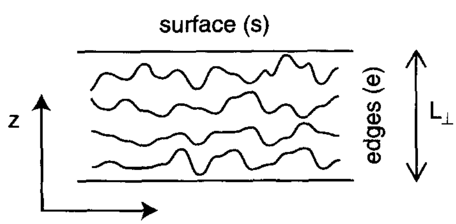

Fig. 1. Bundle of strings between two rigid boundaries or surfaces. The probability of local contacts between strings is different deep inside and at the edges of the bundle. Also, local contacts are less frequent close to the rigid surfaces.

2.2. Periodic and free boundary conditions

Usually, one wants to study systems with periodic boundary conditions in the lateral x-direction (which corresponds to the time-direction in the corresponding quantum-mechanical system) in order to suppress the influence of these boundaries. In this case, the probability distribution for the string positions is proportional to the *squared* wave function Φ_0^2, and the probability $\mathscr{P}_n(z)$ to find local n-contacts at position z for the first n strings is obtained from

$$\mathscr{P}_n(z) \equiv \int_z^{L_\perp} dl_{n+1} \int_{l_{n+1}}^{L_\perp} dl_{n+2} \dots [\Phi_{0,n}(z; l_{n+1}, \dots, l_N)]^2 . \tag{3}$$

The probability to find local n-contacts at position z for *any* subset of the N strings is equal to $(N-n+1)\mathscr{P}_n(z)$.

In numerical work, on the other hand, it is often convenient to use free boundary conditions in the x-direction. The probability distribution for the free edges (or ends) of the strings is then proportional to Φ_0 itself, see, e.g., Ref. [15], and the probability $\mathscr{P}_n^{(e)}(z)$ to find local n-contacts of the free edges is

$$\mathscr{P}_n^{(e)}(z) \equiv \int_z^{L_\perp} dl_{n+1} \int_{l_{n+1}}^{L_\perp} dl_{n+2} \dots c_N L_\perp^{-N/2} \Phi_{0,n}(z; l_{n+1}, \dots, l_N) , \tag{4}$$

where c_N is a $L_\perp$-independent coefficient.

2.3. Contact probabilities away from the surfaces

We will now consider the limit of small $a_k/L_\perp$ in $\Phi_{0,n}$ as given by (2) and thus expand this quantity in powers of $a_k/L_\perp$. As long as z is not close to one of the two surfaces at $z=0$ and $z=L_\perp$, this expansion will contain all powers $(a_k/L_\perp)^m$ including the constant $(a_k/L_\perp)^0$. However, no power can occur twice in the same term since Φ_0 must vanish if $a_i = a_j$ for any pair (i,j). This together with the scaling form (1) for the ground-state wave function implies that the leading terms of the expansion are given by

$$\Phi_{0,n} \approx L_\perp^{-N/2} \sum_\sigma (a_{\sigma(1)}/L_\perp)^0 (a_{\sigma(2)}/L_\perp)^1 \dots (a_{\sigma(n)}/L_\perp)^{n-1} f_\sigma \tag{5}$$

for small $a_k/L_\perp$, where one sums over all permutations σ of $(1,2,\dots,n)$, and the functions f_σ depend on $z/L_\perp$ and on the remaining displacement fields $l_k/L_\perp$ with $n+1 \leqslant k \leqslant N$.

It then follows from (3), which applies to periodic boundary conditions in the x-direction that the probability $\mathscr{P}_n(z)$ to find a local n-contact at position z scales as $\mathscr{P}_n(z) \sim L_\perp^{-n^2}$. Therefore, the probability to find such a contact at *any* position z

with $0<z<L_\perp$ is given by

$$\mathscr{P}_n \sim L_\perp \mathscr{P}_n(z) \sim 1/L_\perp^{n^2-1} \sim 1/\ell^{n^2-1} \quad \text{for large } \ell\,, \tag{6}$$

where the relation $L_\perp = (N+1)\ell$ has been used. This behaviour also applies (i) to the necklace model in which one considers the reunion of n walkers [16,17] (ii) to strings which can partially intersect one another as has been explicitly shown for $n=2$ [18,19], and (iii) to periodic boundary conditions in the z-direction [20,21].

In general, the behaviour as given by (6) is valid as long as the string segments are not affected by boundaries. On the other hand, the probability $\mathscr{P}_n^{(e)}(z)$ for local contacts of the free edges at position z is obtained when (5) is inserted into (4). One then finds that $\mathscr{P}_n^{(e)}(z) \sim L_\perp^{-(n^2+n)/2}$ which implies

$$\mathscr{P}_n^{(e)} \sim L_\perp \mathscr{P}_n^{(e)}(z) \sim 1/L_\perp^{(n^2+n-2)/2} \sim 1/\ell^{(n^2+n-2)/2} \quad \text{for large } \ell\,. \tag{7}$$

For $n=2$, one has $\mathscr{P}_2 \sim 1/\ell^2$ which also applies to two strings which can partially intersect one another [18]. Since $\mathscr{P}_n^{(e)} \gg \mathscr{P}_n$, contacts of the free edges are more frequent than those in the bulk.

2.4. Contact probabilities close to the surfaces

At the surface of the bunch, i.e., for $z=0$ or $z=L_\perp$, the expansion of $\Phi_{0,n}$ as given by (5) does not apply. Indeed, all one-particle eigenfunctions vanish at these z-values and their expansion in powers of a_k involves only *odd* powers of a_k. Therefore, one obtains the behaviour

$$\Phi_{0,n}(z=0) \approx L_\perp^{-N/2} \sum_\sigma (a_{\sigma(1)}/L_\perp)^1 (a_{\sigma(2)}/L_\perp)^3 \ldots (a_{\sigma(n)}/L_\perp)^{2n-1} f'_\sigma \tag{8}$$

for small $a_k/L_\perp$, where the function f'_σ depends on the displacement fields $l_k/L_\perp$ with $n+1 \leqslant k \leqslant N$. If one inserts this form into (3), one obtains the scaling behaviour [22]

$$\mathscr{P}_n^{(s)} \equiv \mathscr{P}_n(z=0) \sim 1/L_\perp^{2n^2+n} \sim 1/\ell^{2n^2+n} \quad \text{for large } \ell\,, \tag{9}$$

which describes the probability to find a local n-contact directly in front of the surface. In addition, it now follows from (8) and (4) that the probability $\mathscr{P}_n^{(e,s)}$ for a local contact of n string edges directly adjacent to the rigid surface is found to behave as

$$\mathscr{P}_n^{(e,s)} \equiv \mathscr{P}_n^{(e)}(z=0) \sim 1/L_\perp^{n^2+n} \sim 1/\ell^{n^2+n} \quad \text{for large } \ell\,. \tag{10}$$

2.5. Contact exponents

In summary, all contact probabilities of the strings decay as inverse power laws $\sim 1/\ell^{2\zeta_n}$ with the mean separation ℓ, but the values of the contact exponents ζ_n are different for contacts which are close to or far away from the boundaries of the bunch. Using the analogies between the scaling properties of strings and those of fluid membranes, one predicts that the scaling laws (6), (7), (9), and (10) also apply to the corresponding contact probabilities of membranes. In general, the contact exponents ζ_n are defined via

$$\mathscr{P}_n \sim 1/\xi_{\parallel}^{\zeta_n} \sim 1/\ell^{\zeta_n/\zeta}\,, \tag{11}$$

i.e., in terms of the longitudinal correlation length $\xi_{\parallel} \sim \ell^{1/\zeta}$ which involves the roughness exponent ζ. For strings and fluid membranes, one has $\zeta = \frac{1}{2}$ and $\zeta = 1$, respectively. This implies that the contact exponents $\zeta_{n,M}$ and $\zeta_{n,S}$ for membranes and strings are related by

$$\zeta_{n,M} = 2\zeta_{n,S}\,. \tag{12}$$

Note that the probability $\mathscr{P}_2$ for pair contacts deep inside the bundle or bunch scales in the same way as the probability $\mathscr{P}_1^{(s)}$ for contacts of one string or membrane with the surface: $\mathscr{P}_2 \sim \mathscr{P}_1^{(s)} \sim 1/\ell^3$. Likewise, one has $\mathscr{P}_2^{(e)} \sim \mathscr{P}_1^{(e,s)} \sim 1/\ell^2$. These two scaling relations will now be checked and confirmed by Monte Carlo simulations.

3. Monte Carlo simulations for two membranes

Thus, consider two membranes with bending rigidities κ_1 and κ_2 which are pushed together by the pressure P and which experience hard-wall interactions. Their displacement fields are denoted by $l_i(\boldsymbol{x})$ with $i = 1, 2$. Separating off the centre of mass coordinate, one obtains the effective Hamiltonian

$$\mathscr{H}\{l\} = \int d^2x \left[\frac{1}{4}\kappa(\nabla^2 l)^2 + Pl + V_{hw}(l)\right] \tag{13}$$

for the separation field $l \equiv l_2 - l_1$ with $\kappa \equiv 2\kappa_1\kappa_2/(\kappa_1 + \kappa_2)$. Note that $\kappa = \kappa_1$ for two identical membranes and that $\kappa = 2\kappa_1$ for one membrane in front of a rigid surface. The hard-wall interaction is defined by $V_{hw}(l) = 0$ for $l > 0$ and $V_{hw}(l) = \infty$ for $l < 0$.

In the Monte Carlo work, the spatial coordinate $\boldsymbol{x}$ is discretized using a square lattice with lattice constant Δx, and the discretized model is expressed in terms of the dimensionless displacement field $z \equiv (\kappa/T)^{1/2}\, l/\Delta x$ and the dimensionless pressure $p \equiv \Delta x^3(\kappa T)^{-1/2}P$ as described in previous work. [1] Using the standard Metropolis algorithm, we typically did 10^6 MC steps per site on lattices with up to 80×80 sites.

First, the system was studied with periodic boundary conditions in the lateral $\boldsymbol{x}$-direction. In the limit of small p, both the mean separation $\langle z\rangle$ and the roughness $\xi_{\perp,z} \equiv (\langle z^2\rangle - \langle z\rangle^2)^{1/2}$ scale as $\langle z\rangle \sim \xi_{\perp,z} \sim 1/p^{\psi}$ with $\psi = \frac{1}{3}$ as shown previously. In the new simulations, we measured the whole probability distribution $\mathscr{P}(z)$ for different values of the reduced pressure p. From this distribution, the contact probability $\mathscr{P}_2$ was obtained via $\mathscr{P}_2 \equiv \mathscr{P}(z < z_h)$ for some fixed length scale z_h which was varied between $z_h = 0.01$ and $z_h = 0.1$ (for comparison, we note that $\langle z\rangle \simeq 2.9$ at $p = 0.01$).

[1] Compared to [4], the rescaling differs by a factor of $\sqrt{2}$ since κ differs by a factor of 2.

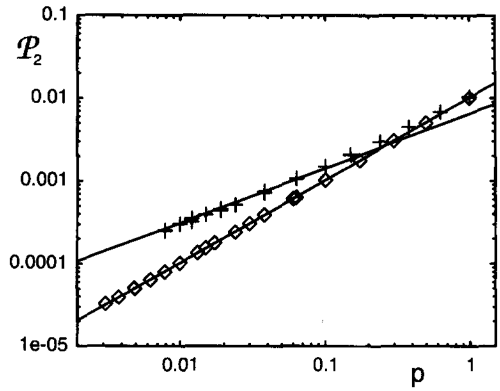

Fig. 2. Monte Carlo data for the contact probability $\mathscr{P}_2$ as a function of the reduced pressure p: the symbols ($\diamond$) are for periodic boundary conditions along the edges of the membrane segment, whereas the symbols (+) correspond to free boundary conditions on two opposite edges. In the latter case, $\mathscr{P}_2$ is measured only at the free edges. In this and all other figures, the error bars are smaller than the size of the symbols.

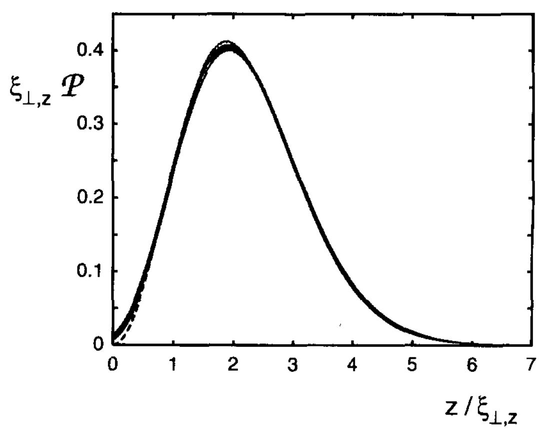

Fig. 3. Rescaled distribution function $\xi_{\perp,z}\mathscr{P}$ for membranes as a function of the rescaled membrane separation $z/\xi_{\perp,z}$: Monte Carlo data for reduced pressure $p = 0.0031, 0.0038, 0.0049, 0.0063, 0.0079, 0.01$ all of which collapse onto one scaling function. The data is represented by lines because the resolution in $z/\xi_{\perp,z}$ is smaller than 0.008. The dashed line as obtained for strings in the continuum limit deviates slightly from the membrane data for small values of $z/\xi_{\perp,z}$.

The data for $z_b = 0.01$ are displayed in Fig. 2. From these data, one obtains the power law $\mathscr{P}_2 \sim p^{\psi\zeta_2}$ with the estimate $\psi\zeta_2 = 0.999 \pm 0.003$. Using the known value $\psi = \frac{1}{3}$, one arrives at the contact exponent $\zeta_2 = 2.997 \pm 0.009$ which is in very good agreement with the value $\zeta_2 = 3$ as predicted from the string analogy. We have checked that this value does not depend on the choice of z_b.

The probability distribution $\mathscr{P}(z)$ should exhibit the scaling form $\mathscr{P}(z) \approx \xi_{\perp,z}^{-1} \times \Omega(z/\xi_{\perp,z})$. The rescaled distribution function $\xi_{\perp,z}\mathscr{P}(z)$ as measured in the simulations is displayed in Fig. 3 as a function of $z/\xi_{\perp,z}$ for six different values of p. For

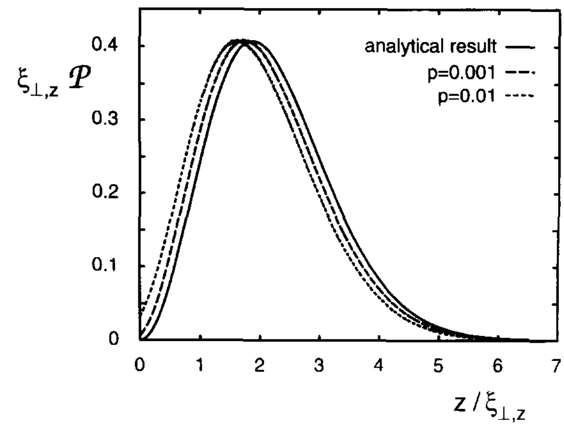

Fig. 4. Rescaled distribution function $\xi_{\perp,z}\mathscr{P}$ for strings: Monte Carlo data for the reduced pressures $p=10^{-2}$ and $p=10^{-3}$ for strings of $N=200$ and $N=400$ points, respectively. The full line corresponds to the analytical solution as obtained in the continuum limit.

comparison, the corresponding quantity for two strings as obtained from the transfer-matrix method in the continuum limit is also displayed in Fig. 3. Inspection of this figure shows that the membrane data collapse very well onto the string curve. A small deviation is obtained for small z but this reflects the effect of the finite lattice constant. Indeed, simulation data for two strings as obtained for a discretized model exhibit the same deviation from the continuum limit, see Fig. 4.

Secondly, we performed simulations of membranes with free boundary conditions on two opposite edges and periodic boundary conditions on the two remaining edges. On the free edges, we only took into account the curvature parallel to the edge. The results for the contact probability of the free edges are also displayed in Fig. 2. In the limit of small p, the data show the scaling behaviour $\mathscr{P}_2^{(e)} \sim p^{\psi\zeta_2^{(e)}}$ with $\psi\zeta_2^{(e)}=0.66\pm0.01$ as estimated from a least-squares fit using the data points with $0.0079 \leqslant p \leqslant 0.038$. In addition, the simulation data for the roughness $\xi_{\perp,z}$ measured at the free edges of the membrane and displayed in Fig. 5 are well fitted by the power law $\xi_{\perp,z} \sim p^{-\psi}$ with $\psi=0.37\pm0.04$, which is still consistent with $\psi=\frac{1}{3}$. Thus, local pair contacts of the membrane edges are found to behave as $\mathscr{P}_2^{(e)} \sim 1/\ell^{\zeta_2^{(e)}}$ with the contact exponent $\zeta_2^{(e)}=1.8\pm0.2$ which is again consistent with the string value.

In summary, the MC data for membranes discussed here confirm the scaling laws as obtained by analogy with the string behaviour. First, the probability $\mathscr{P}_2$ for pair contacts scales as $\mathscr{P}_2 \sim 1/\ell^{\zeta_2}$ and the observed contact exponent ζ_2 is in very good agreement with the value $\zeta_2=3$ as obtained from the scaling analogy. This shows explicitly that the prediction $\zeta_2=2$ as obtained from the naive collision picture is wrong. Secondly, the pair contacts of free membrane edges are more frequent than those away from the boundaries; these edge contacts are governed by the contact exponent $\zeta_2^{(e)}$ whose measured value is in fair agreement with the value $\zeta_2^{(e)}=2$ obtained from the string analogy.

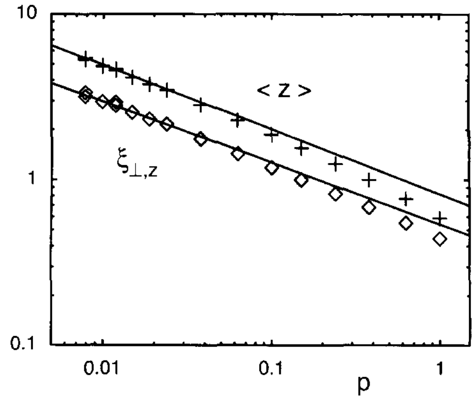

Fig. 5. Mean separation $\langle z \rangle$ and roughness $\xi_{\perp,z}$ as a function of the reduced pressure p for interacting membranes with free boundary conditions at two opposite edges as measured at these edges. The lines represent a fit to the data points with the six smallest p-values.

Thus, the scaling laws for the contact probabilities as given by (6), (7), (9), and (10) which have been obtained for local contacts of n strings should apply to n fluid membranes as well. Inspection of these scaling laws shows that the contact exponents ζ_n have, for any n, different values away from the boundaries and close to the boundaries of the system. This implies that the contact probabilities satisfy the inequalities $\mathscr{P}_n^{(e)} \gg \mathscr{P}_n \gg \mathscr{P}_n^{(e,s)} \gg \mathscr{P}_n^{(s)}$, where the superscripts (e) and (s) denote the edge and the rigid surface as before. Therefore, local contacts within the bundle or bunch are less frequent than those between the edges which reflects the enhanced edge fluctuations. In addition, a rigid surface acts to suppress these contacts.

4. Intermediate fluctuation regime

If two strings interact with a repulsive potential which decays as W/l^2 for large l, their contact exponent ζ_2 depends continuously on the amplitude W. Analogous behaviour is expected for interacting membranes.

In order to investigate this case, we have also performed MC simulations for membranes interacting with such a long-ranged potential. As before, the discretized model is expressed in terms of the dimensionless deplacement field $z = (\kappa/T)^{1/2} l/\Delta x$. The potential $V(l)$ is rescaled to $\tilde{V}(z) \equiv w/z^2$ with $w = (\kappa/T^2)W$. This potential $\tilde{V}(z)$ has a singularity at $z = 0$. Therefore, it would be difficult to measure the contact probability in a simulation using $\tilde{V}(z)$. Since the critical behaviour should only depend on the long-range part of the potential, we use two potentials with modified short-distance behaviour: (i) the cut-off potential $\tilde{V}_c(z) \equiv w/z^2$ for $z > z_b$ and $\tilde{V}_c(z) \equiv w/z_b^2$ for $z \leqslant z_b$, and (ii) the shifted potential $\tilde{V}_l(z) \equiv w/(z + z_b)^2$.

The results are shown in Fig. 6. For $w = 0.01$ the fit of the data to $\mathscr{P}_2 \sim p^{\alpha}$ yields $\alpha = 1.10 \pm 0.01$ for the cut-off potential $\tilde{V}_c$ (marked with $\diamond$) and $\alpha = 1.07 \pm 0.01$ for the

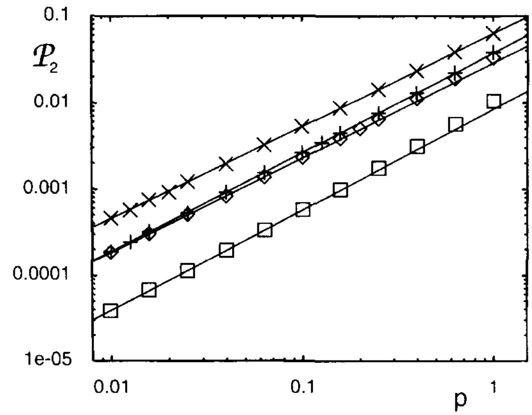

Fig. 6. Monte Carlo data for the contact probability $\mathscr{P}_2$ as a function of the reduced pressure p in the presence of a repulsive $1/l^2$ potential. We show data for the potential strength $w=0.01$ and $w=0.02$. In each case, we used two potentials with different short-distance behaviour. The symbol ($\diamond$) corresponds to $w=0.01$ and $\tilde{V}_c$, the symbol $\times$ to $w=0.01$ and $\tilde{V}_t$, the symbol ($\square$) to $w=0.02$ and $\tilde{V}_c$, and the symbol $+$ to $w=0.02$ and $\tilde{V}_t$.

shifted potential $\tilde{V}_t$ (marked with $\times$). In both cases, we used $z_h=0.1$. The roughness $\xi_{\perp,z}$ scales as $\xi_{\perp,z} \sim p^{-\psi}$ with $\psi=0.31 \pm 0.01$ for both potentials. This is almost consistent with $\psi=\frac{1}{3}$ as obtained by minimizing the superposition of the direct interaction and the fluctuation-induced repulsion, i.e., $Pl+W/l^2+c_{Fl}T^2/\kappa l^2$ and assuming $\xi_\perp \sim \langle l \rangle$. The deviation of ψ from the predicted value $\frac{1}{3}$ is due to the fact that the asymptotic behaviour for small p is not yet fully reached (see the data in [7]). Taking $\alpha=1.09$ and $\psi=\frac{1}{3}$, we find the contact exponent $\zeta_2 \simeq 3.3$ for $w=0.01$.

For $w=0.02$, we find the values $\alpha=1.17 \pm 0.01$ for the potential $\tilde{V}_c$ (marked with $\square$), and $\alpha=1.15 \pm 0.01$ for $\tilde{V}_t$ (marked with $+$) with $z_h=0.1$ in both cases. We obtain the exponents $\psi=0.30 \pm 0.01$ and $\psi=0.31 \pm 0.01$ for $\tilde{V}_c$ and $\tilde{V}_t$, respectively. Taking again $\psi=1/3$, we obtain $\zeta_2 \simeq 3.5$.

For strings interacting with a direct interaction of the form W/l^2, with $W>0$ for large l, one obtains the contact probability $\mathscr{P}_2 \sim \xi_\perp^{-2\zeta_2}$ with $\zeta_2 = 1+\sqrt{1/4+w}$ and $w=\sigma W/T^2$ [1]. If one assumes that the analogy between membranes and strings also holds in this case, then this implies a contact exponent

$$\zeta_2 = 2+\sqrt{1+c_w w} \tag{14}$$

for membranes where c_w is a constant and $w=(\kappa/T^2)W$. Together with relation (14) our results lead to the rough estimate $c_w \simeq 60$.

In summary, our data indicate that the contact exponent ζ_2 depends on the amplitude W, when a W/l^2 potential is present. More extensive investigations remain to be done in order to check the functional form as given by (14).

5. Related problems

Finally, let us briefly mention some related problems. For bundles of strings in three dimensions, the steric hindrance of the strings is strongly reduced and the contact probabilities $\mathscr{P}_n$ should scale as $\sim 1/\ell^{2(n-1)}$ for intersecting strings [21]. Local contacts have also been studied for bunches of surfaces with tension [25] and for semi-flexible polymers [26,27]. Another non-trivial problem is the bunches of polymerized membranes which have a reduced roughness exponent $\zeta < 1$ compared to fluid membranes [23]. At present, the best estimate is $\zeta \simeq 0.59$ [24]. It has been recently proposed [22] that the corresponding contact exponent ζ_2 should satisfy the scaling relation $\zeta_2 = 2 + \zeta$ which implies $\zeta_2 \simeq 2.59$. In addition, edge contacts should again be governed by a different contact exponent $\zeta_2^{(e)} < \zeta_2$. It would be interesting to confirm these predictions by computer simulations.

Acknowledgements

We thank R. Bundschuh for stimulating interactions. R.L. takes this opportunity to thank Ben Widom for his kind hospitality at Cornell and for much advice and many helpful discussions.

References

[1] R. Lipowsky, in: R. Lipowsky, E. Sackmann (eds.), Structure and Dynamics of Membranes, Handbook of Biological Physics, vol. 1, Elsevier, Amsterdam, 1995, pp. 521–602.
[2] A. Cowley, N. Fuller, R. Rand, V. Parsegian, Biochemistry 17 (1978) 3163.
[3] W. Helfrich, Z. Naturf. 33a (1978) 305.
[4] R. Lipowsky, B. Zielinska, Phys. Rev. Lett. 62 (1989) 1572.
[5] G. Gompper, D. Kroll, Europhys. Lett. 9 (1989) 59.
[6] W. Janke, H. Kleinert, M. Meinhart, Phys. Lett. B 217 (1989) 525.
[7] R. Netz, R. Lipowsky, Europhys. Lett. 29 (1995) 345.
[8] D. Roux, C. Safinya, in: J. Meunier, D. Langevin, N. Boccara (eds.), Physics of Amphiphilic Layers, Springer Proceedings in Physics, vol. 21, Springer, Berlin, 1987, pp. 138–144.
[9] G. Porte, P. Bassereau, J. Marignan, R. May, in: J. Meunier, D. Langevin, N. Boccara (eds.), Physics of Amphiphilic Layers, Springer Proceedings in Physics, vol. 21, Springer, Berlin, 1987, pp. 145–152.
[10] E. Gruber, W. Mullins, J. Phys. Chem. Solids 28 (1967) 875.
[11] V.A. Pokrovskii, A.L. Talanov, Sov. Phys. JETP 51 (1980) 134.
[12] P.-G. de Gennes, J. Chem. Phys. 48 (1968) 2257.
[13] J. Villain, P. Bak, J. Phys. (Paris) 42 (1981) 657.
[14] H.B. Thacker, Rev. Mod. Phys. 53 (1981) 253.
[15] G. Forgacs, R. Lipowsky, T. Nieuwenhuizen, in: C. Domb, J. Lebowitz (eds.), Phase Transitions and Critical Phenomena, vol. 14, Academic Press, London, 1991, pp. 136–363.
[16] D. Huse, M. Fisher, Phys. Rev. B 29 (1984) 239.
[17] M. Fisher, J. Stat. Phys. 34 (1984) 667.
[18] C. Hiergeist, Diploma Thesis, University of Cologne, 1994.
[19] M. Lässig, R. Lipowsky, Phys. Rev. Lett. 70 (1993) 1131.
[20] M. Lässig, Phys. Rev. Lett. 73 (1994) 561.
[21] M. Lässig, R. Lipowsky, in: H. van Beijeren (eds.), Fundamental Problems in Statistical Mechanics VIII, North-Holland, Amsterdam, 1994, pp. 169–206.

[22] R. Lipowsky, Z. Phys. B 97 (1995) 193.
[23] D. Nelson, L. Peliti, J. Phys. (Paris) 48 (1987) 1085.
[24] P.L. Doussal, L. Radzihovsky, Phys. Rev. Lett. 69 (1992) 1209; Z. Zhang, H.T. Davis, D.M. Kroll, Phys. Rev. E 53 (1996) 1422.
[25] A. Volmer, Diploma Thesis, University of Cologne, 1995; A. Volmer, U. Seifert, R. Lipowsky, in preparation.
[26] T.W. Burkhardt, J. Phys. A 26 (1993) L1157.
[27] R. Bundschuh, Ph.D. Thesis, University of Potsdam, 1996; R. Bundschuh, M. Lässig, R. Lipowsky, in preparation.